# $^3P_2$-$^3F_2$ pairing in neutron matter with modern nucleon-nucleon potentials

M. Baldo,[1] Ø. Elgarøy,[2] L. Engvik,[2] M. Hjorth-Jensen,[3] and H.-J. Schulze[1]
[1]*Sezione INFN, Università di Catania, Corso Italia 57, I-95129 Catania, Italy*
[2]*Department of Physics, University of Oslo, N-0316 Oslo, Norway*
[3]*Nordita, Blegdamsvej 17, DK-2100 Copenhagen Ø, Denmark*
(Received 29 June 1998)

We present results for the $^3P_2$-$^3F_2$ pairing gap in neutron matter with several realistic nucleon-nucleon potentials, in particular with recent phase-shift-equivalent potentials. We find that their predictions for the gap cannot be trusted at densities above $\rho \approx 1.7\rho_0$, where $\rho_0$ is the saturation density for symmetric nuclear matter. In order to make predictions above that density, potential models which fit the nucleon-nucleon phase shifts up to about 1 GeV are required. [S0556-2813(98)06010-5]

PACS number(s): 26.60.+c, 21.30.−x, 21.65.+f, 97.60.Jd

## I. INTRODUCTION

The presence of neutron superfluidity in the crust and the inner part of neutron stars is one of the features that is considered well established in the physics of these compact stellar objects. At low density, and therefore in the outer part of a neutron star, the neutron superfluidity should be mainly in the $^1S_0$ channel. At higher density, the nuclei in the crust dissolve, and one expects a region consisting of a quantum liquid of neutrons and protons in beta equilibrium. The proton contaminant should be superfluid in the $^1S_0$ channel, while neutron superfluidity is expected to occur mainly in the coupled $^3P_2$-$^3F_2$ two-neutron channel. In the core of the star any superfluid phase should finally disappear.

The presence of two different superfluid regimes is suggested by the known trend of the nucleon-nucleon (*NN*) phase shifts in each scattering channel. In both the $^1S_0$ and $^3P_2$-$^3F_2$ channels the phase shifts indicate that the *NN* interaction is attractive. In particular for the $^1S_0$ channel, the occurrence of the well-known virtual state in the neutron-neutron channel strongly suggests the possibility of a pairing condensate at low density, while for the $^3P_2$-$^3F_2$ channel the interaction becomes strongly attractive only at higher energy, which therefore suggests a possible pairing condensate in this channel at higher densities. In recent years the BCS gap equation has actually been solved with realistic interactions, and the results confirm these expectations.

The $^1S_0$ neutron superfluid is relevant for phenomena that can occur in the inner crust of neutron stars, like the formation of glitches, which seem to be related to vortex pinning of the superfluid phase in the solid crust [1]. The results of different groups are in close agreement on the $^1S_0$ pairing gap values and on its density dependence, which shows a peak value of about 3 MeV at a Fermi momentum close to $k_F \approx 0.8\,\mathrm{fm}^{-1}$ [2–5]. All these calculations adopt the bare *NN* interaction as the pairing force, and it has been pointed out that screening by the medium of the interaction could strongly reduce the pairing strength in this channel [5–7]. However, the issue of the many-body calculation of the pairing effective interaction is a complex one and still far from a satisfactory solution.

Precise knowledge of the $^3P_2$-$^3F_2$ pairing gap is of paramount relevance for, e.g., the cooling of neutron stars, and different values correspond to drastically different scenarios for the cooling process [8]. Unfortunately, only few and partly contradictory calculations of this quantity exist in the literature, even at the level of the bare *NN* interaction [9–13]. However, when comparing the results, one should note that the *NN* potentials used in these calculations are not phase-shift equivalent; i.e., they do not predict exactly the same *NN* phase shifts. Furthermore, for the interactions used in Refs. [9–12] the predicted phase shifts do not agree accurately with modern phase-shift analyses, and the fit of the *NN* data has typically $\chi^2/\mathrm{datum} \approx 3$. During the last years, progress has been made not only in the accuracy and the consistency of the phase-shift analysis, but also in the fit of realistic *NN* potentials to these data. As a result, several new *NN* potentials have been constructed which fit the world data for *pp* and *np* scattering below 350 MeV with high precision. Potentials like the recent Argonne $V_{18}$ [14], the CD-Bonn [15], or the new Nijmegen potentials [16] yield a $\chi^2$/datum of about 1 and may be called phase-shift equivalent.

Our aim in this paper is to compare the predictions of the new potentials for the $^3P_2$-$^3F_2$ gap in neutron matter. We will also, for the sake of completeness, include results with some of the ''old'' interactions, namely, the Paris [17], Argonne $V_{14}$ [18], and Bonn B [19] potentials. The main focus will, however, be on the new, phase-shift-equivalent potentials, and whether the improved accuracy in the fits to the *NN* scattering data leads to better agreement in the predictions for the $^3P_2$-$^3F_2$ energy gap. If differences are found, we try to trace them back to features of the *NN* potentials. To be able to do so, we will keep the many-body formalism as simple as possible. First of all, we will use the bare *NN* interaction as a kernel in the gap equations, and thus neglect higher-order contributions from, e.g., medium polarization effects. The in-medium single-particle energies will be calculated in the Brueckner-Hartree-Fock (BHF) approximation, but we will also use free single-particle energies, because this makes the comparison of the results with the various potentials more transparent, since any differences are then solely due to differences in the $^3P_2$-$^3F_2$ wave of the potentials. We think it is useful to try to understand the results at the simplest level of many-body theory before pro-

 

ceeding to include more complicated effects in the description of $^3P_2$-$^3F_2$ pairing. As we will demonstrate, progress in the construction of *NN* interactions is necessary before the $^3P_2$-$^3F_2$ energy gap can be calculated reliably from microscopic many-body theory.

This work falls into six sections. The equations for solving the pairing gap are briefly reviewed in the next section, while in Sec. III we discuss the reliability of various numerical approaches to the solution of the pairing gap. Features of the various nucleon-nucleon interaction models employed are presented in Sec. IV, while our results for the pairing gap with these potentials are discussed in Sec. V. Finally, we summarize our findings in Sec. VI.

## II. GAP EQUATION FOR THE $^3P_2$-$^3F_2$ CHANNEL

The gap equation for pairing in nonisotropic partial waves is in general more complex than in the simplest *s*-wave case, in particular in neutron and nuclear matter, where the tensor interaction can couple two different partial waves [11,20]. This is indeed the situation for the $^3P_2$-$^3F_2$ neutron channel. In order to achieve a simplified, yet accurate, numerical treatment, we use in this work the angle average approximation explained in this section.

For the sake of a clear presentation, we disregard for the moment the spin degrees of freedom and the tensor interaction. Then, we start with the Gorkov equations [21], which involve the propagator $G(\boldsymbol{k},\omega)$, the anomalous propagator $F(\boldsymbol{k},\omega)$, and the gap function $\Delta(\boldsymbol{k})$:

$$\begin{pmatrix} \omega-\epsilon(\boldsymbol{k}) & -\Delta(\boldsymbol{k}) \\ -\Delta^{\dagger}(\boldsymbol{k}) & \omega+\epsilon(\boldsymbol{k}) \end{pmatrix}\begin{pmatrix} G \\ F^{\dagger} \end{pmatrix}(\boldsymbol{k},\omega)=\begin{pmatrix} 1 \\ 0 \end{pmatrix}, \tag{1}$$

where $\epsilon(\boldsymbol{k})=e(\boldsymbol{k})-\mu$, $\mu$ being the chemical potential and $e(\boldsymbol{k})$ the single-particle spectrum. The quasiparticle energy $E(\boldsymbol{k})$ is the solution of the corresponding secular equation and is given by

$$E(\boldsymbol{k})^2=\epsilon(\boldsymbol{k})^2+|\Delta(\boldsymbol{k})|^2. \tag{2}$$

The anisotropic gap function $\Delta(\boldsymbol{k})$ is to be determined from the gap equation

$$\Delta(\boldsymbol{k})=-\sum_{\boldsymbol{k}'}\langle \boldsymbol{k}|V|\boldsymbol{k}'\rangle\frac{\Delta(\boldsymbol{k}')}{2E(\boldsymbol{k}')}. \tag{3}$$

The angle-dependent energy denominator in this equation prevents a straightforward separation into the different partial-wave components by expanding the potential

$$\langle \boldsymbol{k}|V|\boldsymbol{k}'\rangle=4\pi\sum_{l}(2l+1)P_l(\hat{\boldsymbol{k}}\cdot\hat{\boldsymbol{k}}')V_l(k,k') \tag{4}$$

and the gap function

$$\Delta(\boldsymbol{k})=\sum_{l,m}\sqrt{\frac{4\pi}{2l+1}}Y_{lm}(\hat{\boldsymbol{k}})\Delta_{lm}(k). \tag{5}$$

However, after performing an angle average approximation for the gap in the quasiparticle energy,

$$|\Delta(\boldsymbol{k})|^2\rightarrow D(k)^2\equiv\frac{1}{4\pi}\int d\hat{\boldsymbol{k}}|\Delta(\boldsymbol{k})|^2=\sum_{l,m}\frac{1}{2l+1}|\Delta_{lm}(k)|^2, \tag{6}$$

the kernels of the coupled integral equations become isotropic, and one can see that the different *m* components become uncoupled and all equal. One obtains the following equations for the partial-wave components of the gap function:

$$\Delta_l(k)=-\frac{1}{\pi}\int_0^{\infty}\frac{V_l(k,k')k'^2\,dk'}{\sqrt{\epsilon(k')^2+[\Sigma_{l'}\Delta_{l'}(k')^2]}}\Delta_l(k'). \tag{7}$$

Note that there is no dependence on the quantum number *m* in these equations; however, they still couple the components of the gap function with different *l* ($^1S_0$, $^3P_0$, $^3P_1$, $^3P_2$, $^1D_2$, $^3F_2$, etc., in neutron matter) via the energy denominator. Fortunately, in practice the different components $V_l$ of the potential act mainly in nonoverlapping intervals in density, and therefore also this coupling can usually be disregarded.

The addition of spin degrees of freedom and of the tensor force does not change the picture qualitatively, and is explained in detail in Refs. [11,20]. The only modification is the introduction of an additional $2\times2$ matrix structure due to the tensor coupling of the $^3P_2$ and $^3F_2$ channels:

$$\begin{pmatrix}\Delta_1\\ \Delta_3\end{pmatrix}(k)=-\frac{1}{\pi}\int_0^{\infty}dk'k'^2\frac{1}{E(k')}\times\begin{pmatrix} V_{11} & -V_{13}\\ -V_{31} & V_{33}\end{pmatrix}(k,k')\begin{pmatrix}\Delta_1\\ \Delta_3\end{pmatrix}(k'), \tag{8a}$$

$$E(k)^2=[e(k)-e(k_F)]^2+D(k)^2, \tag{8b}$$

$$D(k)^2=\Delta_1(k)^2+\Delta_3(k)^2. \tag{8c}$$

Here $e(k)=k^2/2m+U(k)$ are the single-particle energies, as obtained from a Brueckner-Hartree-Fock calculation, where $U(k)$ is the single-particle potential, calculated within the ''continuous choice'' scheme [22]. The quantities

$$V_{ll'}(k,k')=\int_0^{\infty}drr^2j_{l'}(k'r)V_{ll'}(r)j_l(kr)\pi/2 \tag{9}$$

are the matrix elements of the bare interaction in the different coupled channels ($T=1; S=1; J=2; l,l'=1,3$).

It has been shown that the angle average approximation is an excellent approximation to the true solution that involves a gap function with ten components [11,13], as long as one is only interested in the average value of the gap at the Fermi surface, $\Delta_F\equiv D(k_F)$, and not the angular dependence of the gap functions $\Delta_1(\boldsymbol{k})$ and $\Delta_3(\boldsymbol{k})$.

## III. NUMERICAL SOLUTION

The solution of the system of Eqs. (8) is numerically not trivial, especially if the gap turns out to be much smaller than the Fermi energy. This is because of the well-known logarithmic singularity of the BCS equation in the limit of zero pairing gap. In order to control more closely the numerical accuracy, we used in fact three different methods.

One method is similar to the one described in Ref. [2]. We first obtain a separable form of the interaction. Since we need a high accuracy, we directly diagonalize the interaction $V_{ll'}(k,k')$, taken in a discrete grid of momenta $\{k_i\}$, and then we choose the first $n$ eigenvalues $\lambda_m$ with the largest moduli and the corresponding eigenvectors $v_m$. One can then write

$$V_{ll'}(k_i,k_j) \approx \sum_{m=1}^{n} v_m(k_i)\lambda_m v_m(k_j). \tag{10}$$

The gap function can then also be expanded in the same eigenvectors, and the original equations reduce to a set of $2n$ algebraic equations. The latter can be solved for the coefficients of the expansion by iteration, following the scheme described in Ref. [2]. The rank $n$ of the separable form is increased until a high degree of convergence is reached. One advantage of the method is the possibility of using a very fine momentum grid, since the algebraic equations are obtained by numerical integrations, for which extremely accurate interpolation methods can be used. In general, the grid points must be particularly dense in the interval around the Fermi momentum, since there the kernel displays an extremely narrow peak due to the small value of the pairing gap. Furthermore, in general, the convergence in the rank $n$ is fast enough, and therefore the number of coupled equations is never very large. However, the accuracy in the diagonalization procedure decreases with the rank of the matrix and it is difficult to have a precise estimate of the error.

In the second method [23] one starts by solving the gap equation for the case of a constant pairing gap $\overline{\Delta}$ in the denominator. In a discrete momentum grid, this is equivalent to an eigenvalue problem, namely, to find the value of $\overline{\Delta}$ for which the kernel of the gap equation has eigenvalue 1. The corresponding eigenvector is a first estimate of the gap function, with the normalization $\Delta(k_F)=\overline{\Delta}$. It is then inserted in the kernel to solve for the next estimate of $\overline{\Delta}$. In practice this method converges extremely fast (after a few iterations) to the final solution. The advantage of the method is that the original interaction is used, without resorting to a separable form.

The third method is to solve the coupled $^3P_2$-$^3F_2$ gap equations straightforwardly by iteration, starting from some suitable initial approximation to the functions $\Delta_1(k)$ and $\Delta_3(k)$. Also in this method, the interaction is used in its original form. If the interaction has a strong repulsive core, as is the case in the $^1S_0$ channel, this method can be difficult or even impossible to implement. However, the $^3P_2$-$^3F_2$ interaction is relatively weak, and the iteration scheme works well in this channel, provided that a fine momentum grid is used around the Fermi momentum. Details of the numerical implementation of this method are given in Ref. [12].

The comparison of the results obtained with the three methods was quite rewarding. The numerical values of the gap functions were in excellent agreement and hardly distinguishable in all figures presented here. Therefore, in discussing the results we will not specify the method by which they were obtained. We believe that the agreement between the three methods gives enough confidence in the numerical precision of the results.

## IV. *NN* INTERACTIONS

Before discussing the solutions of the coupled $^3P_2$-$^3F_2$ gap equations, we give a short description of the models for the *NN* interaction employed in this paper.

The older models, Paris, Argonne $V_{14}$, and Bonn B, are described in detail in Refs. [17–19]. They all have a $\chi^2$/datum in the range 2–3. The Argonne $V_{14}$ potential is a nonrelativistic, purely local potential. The Paris potential incorporates explicit $\pi$, $2\pi$, and $\omega$ exchange. For the short-range part a phenomenological approach is used. The final potential is parametrized in terms of local Yukawa functions. The Bonn B potential is a one-boson-exchange (OBE) interaction, defined by the parameters of Table A.1 of Ref. [19].

The ''phase-shift-equivalent'' potentials we will employ here are the recent models of the Nijmegen group [16], the Argonne $V_{18}$ [14] potential, and the charge-dependent Bonn potential (CD-Bonn) [15]. In 1993, the Nijmegen group presented a phase-shift analysis of all proton-proton and neutron-proton scattering data below 350 MeV with a $\chi^2$/datum of 0.99 for 4301 data entries [24]. Fitted to this phase-shift analysis, the CD-Bonn potential has a $\chi^2$/datum of 1.03 and the same is true for the Nijm-I and Nijm-II potentials of the Nijmegen group [16]. The Argonne $V_{18}$ potential has a $\chi^2$/datum of 1.09.

All these models are charge dependent. Argonne $V_{18}$ and Nijm-II are nonrelativistic potential models defined in terms of local functions, which are attached to various (nonrelativistic) operators constructed from the spin, isospin, and angular momentum operators of the interacting pair of nucleons. Such approaches to the *NN* potential have traditionally been quite popular since they are numerically easy to use in configuration space calculations. The Nijm-I model is similar to the Nijm-II model, but it includes also a momentum-dependent term [see Eq. (13) of Ref. [16]], which may be interpreted as a nonlocal contribution to the central force. The CD-Bonn potential is based on the relativistic meson-exchange model of Ref. [19] which is nonlocal and cannot be described correctly in terms of local potential functions. Instead, it is represented most conveniently in terms of partial waves.

Thus, the mathematical structure of the modern potentials is quite different, although they all predict almost identical phase shifts within their range of validity. This means that even though the potentials by construction give the same results on shell, their behavior off the energy shell may be quite different. The implications of these differences for the symmetry energy of nuclear matter were discussed in Ref. [25].

In order to illustrate the statements made above, and for a better understanding of the forthcoming results for the pairing gaps, we show in Fig. 1 the predictions of the various potentials for the phase shifts in the $^3P_2$ $(T=1)$ channel. They have been calculated by solving the Lippmann-Schwinger equation as explained in Ref. [26]. The figure shows predictions up to $E_{\rm lab}=1.1$ GeV, but clearly scattering energies above $E_{\rm lab}=350$ MeV amount to uncontrolled extrapolations beyond the intended range of validity of the potential models, which have been fitted to scattering data below 350 MeV only. The plot displays also a scale of equivalent Fermi momenta according to the relation $E_{\rm lab}$

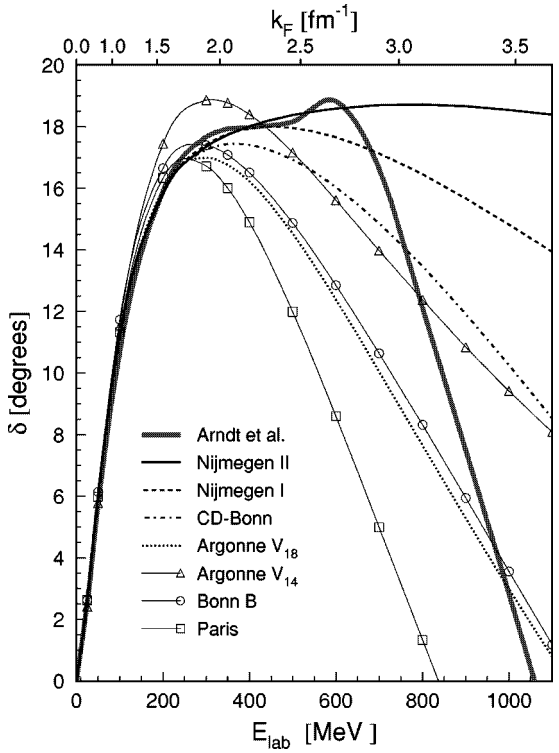


FIG. 1. $^3P_2$ phase-shift predictions of different potentials up to $E_{\rm lab}=1.1$ GeV, compared with the phase-shift analysis of Arndt *et al.* [27]. The ''old'' potentials are denoted by different symbols, the ''modern'' potentials by different line styles.

$=(2k_F)^2/2m$ in order to facilitate the comparison with the pairing gaps presented later. The reader can see that a laboratory energy of 350 MeV corresponds roughly to a Fermi momentum $k_F=2.0$ fm$^{-1}$. Therefore, calculations of the $^3P_2$-$^3F_2$ energy gap at densities above $k_F=2.0$ fm$^{-1}$ will inevitably involve extrapolating the potential models.

In the same figure we also show the empirical $pp$ phase shifts obtained by Arndt *et al.* in a recent phase-shift analysis [27]. Some differences between this phase-shift analysis and the phase shifts calculated with the potentials could be present in the figure, even below 350 MeV, because the potentials are not fitted to the analysis of Arndt *et al.* The modern potentials fit the Nijmegen database [24]; the older ones fit different analyses made in the 1970s and 1980s. Nevertheless, the four modern potentials considered here fit also the analysis of Arndt *et al.* below 350 MeV with a high accuracy, while the old potentials (in particular the $V_{14}$) overshoot the empirical values already at lower scattering energies, due to the fact that they have a higher $\chi^2$/datum than the new models.

In any case, above $E_{\rm lab}=350$ MeV (corresponding to $k_F\approx 2.0$ fm$^{-1}$) sizable differences show up in the predictions of all potentials. The Nijm-II potential fits the phase shifts up to about 600 MeV rather well, but after that it severely overestimates them. This in turn means that the high-momentum components of the $^3P_2$ interaction will be too attractive. Nijm-I does fairly well up to about 500 MeV; from 500 to 700 MeV it underpredicts the phase shifts, while at energies above 700 MeV the results are too high. The CD-Bonn potential gives a similar behavior, but falls faster towards zero at high energies than Nijm-I and -II. Argonne $V_{18}$ gives $^3P_2$ phase shifts below the empirical ones over the whole range $E_{\rm lab}=400-1000$ MeV. The old potentials display similar variations, being generally too repulsive with Paris, the most repulsive of all potentials, followed by Bonn B and Argonne $V_{14}$. In this paper we will further on focus on the new, phase-shift-equivalent potentials, since they are better fitted to modern scattering data. In summary, all potentials give phase shifts which are too attractive above $E_{\rm lab}\approx 700-1000$ MeV, and all except Nijm-II are too repulsive between $\approx 350$ MeV and $\approx 700-1000$ MeV.

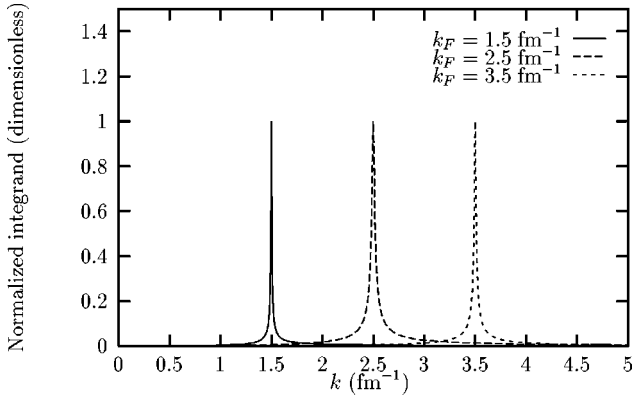


FIG. 2. $^3P_2$ part of the integrand in the gap equations for various densities and with the Nijm-I potential.

## V. RESULTS

Before presenting results for the energy gap, we point out some features of the gap equations which make the trend of the results understandable. In order to make the connection to the *NN* interaction as transparent as possible, we start by discussing the case where the single-particle energies are given by their values in free space, $e(k)=k^2/2m$.

In Fig. 2 we show, for the Nijm-I potential and various values of $k_F$, the function $k^2\Delta_1(k)/E(k)$ involved in the $^3P_2$ component of the gap equations, normalized to unity at $k=k_F$. The behavior of this function was found to be the same for all potentials. Notice that this function is very strongly peaked around $k=k_F$, implying that the diagonal matrix element of the potential at $k=k_F$ gives the most important contribution to $\Delta_1(k_F)$ and $\Delta_3(k_F)$. Also, this figure makes it clear why some care in choosing momentum mesh points for the numerical integrations is needed. The function $k^2\Delta_3(k)/E(k)$ shows a similar, strongly peaked behavior, and thus the gap is largely determined by the matrix elements $V_{11}(k_F,k_F)$, $V_{13}(k_F,k_F)$, and $V_{33}(k_F,k_F)$.

To exemplify this, we have therefore plotted in Fig. 3 the matrix elements for $V_{11}(k_F,k_F)$ and $V_{33}(k_F,k_F)$ as functions of $k_F$ for the various modern potentials used in this work. Up to $k_F\approx 2.0$ fm$^{-1}$ the matrix elements are very similar, but after this point they deviate from each other, in line with the phase-shift predictions shown in Fig. 1: In the $^3P_2$ and $^3F_2$ waves, the $V_{18}$ potential is the most repulsive, followed by the CD-Bonn and the Nijm-I and Nijm-II potentials in that order. Similar conclusions can be reached for the coupled $^3P_2$-$^3F_2$ channel.

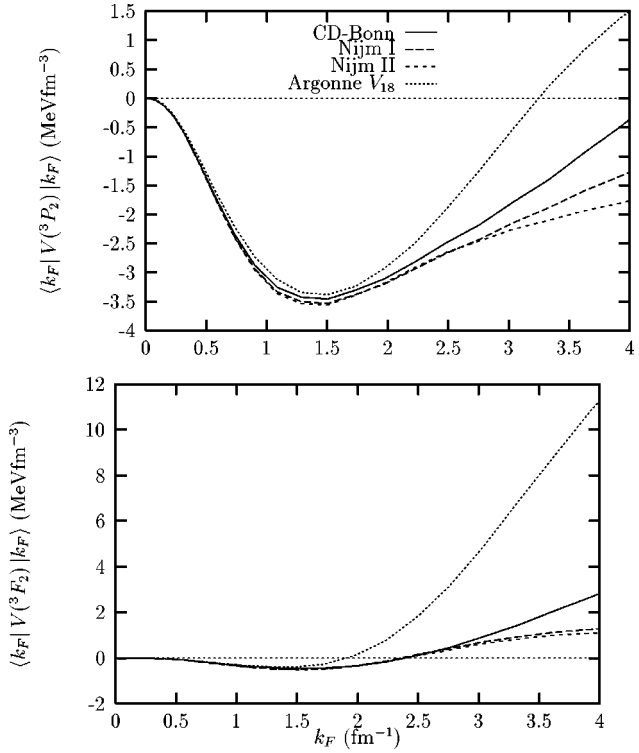


FIG. 3. The diagonal part of the neutron-neutron potential in momentum space [Eq. (9)] for the $^3P_2$ (top panel) and the $^3F_2$ (bottom panel) partial waves obtained with the CD-Bonn, Nijmegen-I and -II, and Argonne $V_{18}$ potentials.

### A. Pairing gaps

Figure 4 contains a comprehensive collection of our results for the pairing gaps with the different potentials. We start with the top part of the figure, which displays the results calculated with free single-particle energies. Differences between the results are therefore solely due to differences in the $^3P_2$-$^3F_2$ matrix elements of the potentials. The plot shows results obtained with the old as well as with the modern potentials. The results [with the notable exception of the Argonne $V_{14}$,[1] which predicts also substantially different $^3P_2$ phase shifts (see Fig. 1)] are in good agreement at densities below $k_F \approx 2.0$ fm$^{-1}$, but differ significantly at higher densities. This is in accordance with the fact that the diagonal matrix elements of the potentials are very similar below $k_F \approx 2.0$ fm$^{-1}$, corresponding to a laboratory energy for free *NN* scattering of $E_{\rm lab} \approx 350$ MeV. This indicates that within this range the good fit of the potentials to scattering data below 350 MeV makes the ambiguities in the results for the energy gap quite small, since, to a first approximation (see the discussion below), the pairing gap can be derived in terms of the phase shifts only.

However, we wish to calculate the gap also at densities above $k_F = 2.0$ fm$^{-1}$. Then we need the various potentials at higher energies, outside of the range where they are fitted to scattering data. Thus there is no guarantee that the results will be independent of the model chosen, and in fact the figure shows that there are considerable differences between their predictions at high densities, following precisely the trend observed in the phase-shift predictions: The Argonne $V_{18}$ is the most repulsive of the modern potentials, followed by the CD-Bonn and Nijmegen-I and -II. Most remarkable are the results obtained with Nijm-II: we find that the predicted gap continues to rise unrealistically even at $k_F \approx 3.5$ fm$^{-1}$, where the purely nucleonic description of matter surely breaks down. From Table I, which contains a compilation of gaps for the various potentials, one sees that the improved fit of the new potentials to scattering data leads to better agreement in their predictions for the gap. Thus, the

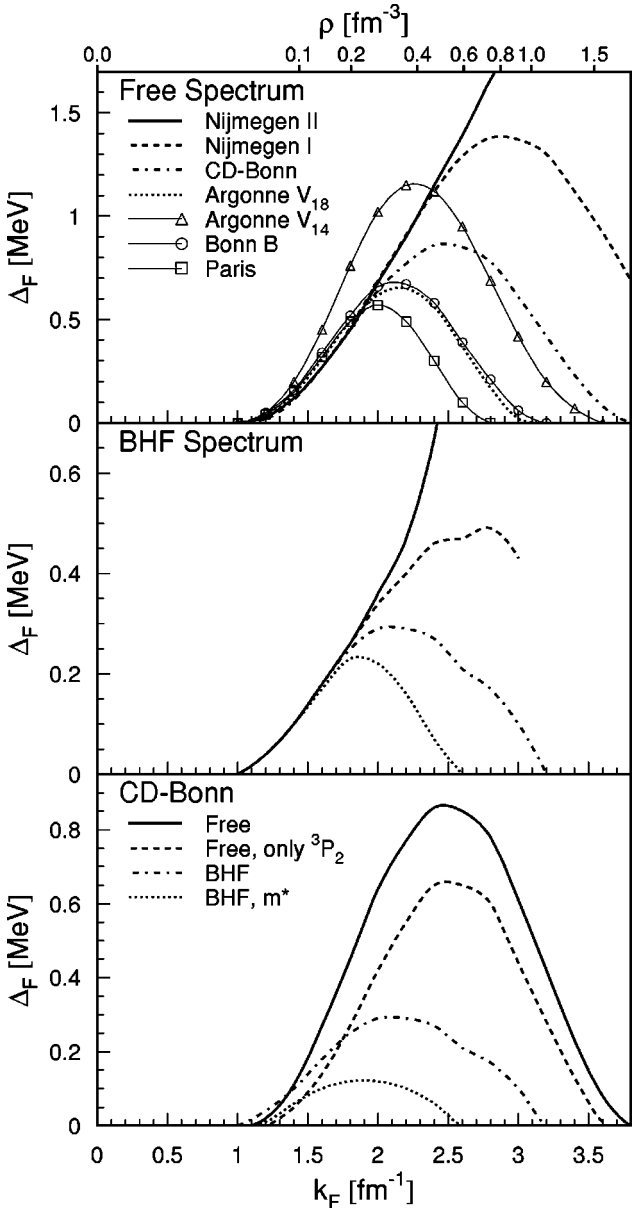


FIG. 4. Top panel: the angle-averaged $^3P_2$-$^3F_2$ gap in neutron matter depending on the Fermi momentum, evaluated with free single-particle spectrum and different nucleon-nucleon potentials. Central panel: the gap evaluated with BHF spectra. Bottom panel: the gap with the CD-Bonn potential in different approximation schemes.

[1] In a previous paper [10] one of the authors (M.B.) has claimed much higher values for the gap with the Argonne $V_{14}$. It has been checked that this was due both to a nonaccurate separable representation of the *NN* potential and to a bug in the computer program for this channel.

TABLE I. Collection of $^3P_2$-$^3F_2$ energy gaps (in MeV) for the various potentials considered in this paper. Free single-particle energies have been used.

| $k_F$ (fm$^{-1}$) | Bonn B | Paris | $V_{14}$ | CD-Bonn | $V_{18}$ | Nijm I | Nijm II |
|---|---|---|---|---|---|---|---|
| 1.2 | 0.05 | 0.04 | 0.05 | 0.03 | 0.04 | 0.03 | 0.03 |
| 1.4 | 0.16 | 0.15 | 0.19 | 0.11 | 0.14 | 0.12 | 0.12 |
| 1.6 | 0.35 | 0.32 | 0.45 | 0.27 | 0.31 | 0.27 | 0.27 |
| 1.8 | 0.52 | 0.49 | 0.75 | 0.45 | 0.49 | 0.47 | 0.45 |
| 2.0 | 0.66 | 0.57 | 1.02 | 0.64 | 0.62 | 0.69 | 0.68 |
| 2.2 | 0.67 | 0.49 | 1.14 | 0.77 | 0.65 | 0.91 | 0.90 |
| 2.4 | 0.58 | 0.30 | 1.13 | 0.86 | 0.56 | 1.12 | 1.15 |
| 2.6 | 0.39 | 0.10 | 0.95 | 0.85 | 0.37 | 1.26 | 1.39 |
| 2.8 | 0.21 | — | 0.70 | 0.78 | 0.17 | 1.38 | 1.66 |
| 3.0 | 0.06 | — | 0.42 | 0.61 | 0.02 | 1.37 | 1.90 |

fact that these potentials have been fit with high precision to the same set of scattering data eliminates some of the ambiguities, and allows one to compare interactions in a way not possible with earlier models.

Since the potentials fail to reproduce the measured phase shifts beyond $E_{\rm lab}=350$ MeV, the predictions for the $^3P_2$-$^3F_2$ energy gap in neutron matter cannot be trusted above $k_F\approx 2.0\,{\rm fm}^{-1}$. Therefore, the behavior of the $^3P_2$-$^3F_2$ energy gap at high densities should be considered as unknown, and cannot be obtained until potential models which fit the phase shifts in the inelastic region above $E_{\rm lab}=350$ MeV are constructed. These potential models need the flexibility to include both the flat structure in the phase shifts above 600 MeV, due to the $NN\rightarrow N\Delta$ channel and the rapid decrease to zero at $E_{\rm lab}\approx 1100$ MeV.

We proceed now to the middle part of Fig. 4, where the results for the energy gap using BHF single-particle energies are shown (see Table II). For details on the BHF calculations, see, e.g., Ref. [22]. From this figure, two trends are apparent: First, the reduction of the in-medium nucleon mass leads to a sizable reduction of the $^3P_2$-$^3F_2$ energy gap, as observed in earlier calculations [9–12]. Second, the new *NN* interactions give again similar results at low densities, while beyond $k_F\approx 2.0\,{\rm fm}^{-1}$ the gaps differ, as in the case with free single-particle energies.

TABLE II. Collection of $^3P_2$-$^3F_2$ energy gaps (in MeV) for the various potentials considered in this paper. BHF single-particle energies have been used.

| $k_F$ (fm$^{-1}$) | Bonn B | Paris | $V_{14}$ | CD-Bonn | $V_{18}$ | Nijm I | Nijm II |
|---|---|---|---|---|---|---|---|
| 1.2 | 0.05 | 0.04 | 0.05 | 0.04 | 0.04 | 0.04 | 0.04 |
| 1.4 | 0.16 | 0.11 | 0.18 | 0.10 | 0.10 | 0.10 | 0.10 |
| 1.6 | 0.34 | 0.22 | 0.38 | 0.18 | 0.17 | 0.18 | 0.18 |
| 1.8 | 0.52 | 0.26 | 0.60 | 0.25 | 0.23 | 0.26 | 0.26 |
| 2.0 | 0.64 | 0.22 | 0.74 | 0.29 | 0.22 | 0.34 | 0.36 |
| 2.2 | 0.65 | 0.14 | 0.75 | 0.29 | 0.16 | 0.40 | 0.47 |
| 2.4 | 0.56 | 0.01 | 0.66 | 0.27 | 0.07 | 0.46 | 0.67 |
| 2.6 | 0.37 | — | 0.42 | 0.21 | — | 0.47 | 0.99 |
| 2.8 | 0.19 | — | 0.23 | 0.17 | — | 0.49 | 1.74 |
| 3.0 | 0.02 | — | 0.08 | 0.11 | — | 0.43 | 3.14 |

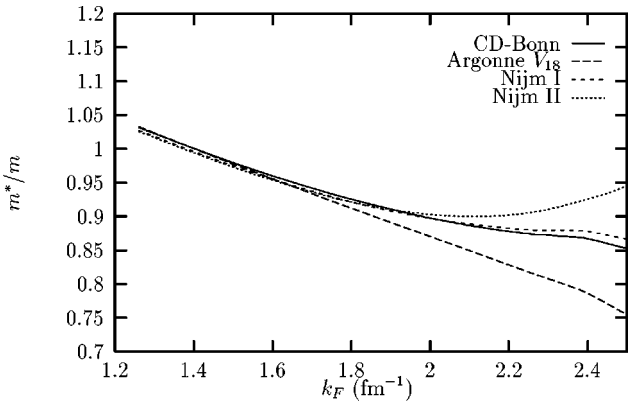


FIG. 5. Effective masses derived from various interactions in the BHF approach.

The single-particle energies at moderate densities obtained from the new potentials are rather similar, particularly in the important region near $k_F$. This is illustrated by a plot, Fig. 5, of the neutron effective mass

$$\frac{m^*}{m}=\left(1+\frac{m}{k_F}\frac{dU}{dk}\bigg|_{k_F}\right)^{-1}, \tag{11}$$

as a function of density. Up to $k_F\approx 2.0\,{\rm fm}^{-1}$ all results agree very closely, but beyond that point the predictions diverge in the same manner as observed for the phase-shift predictions. The differences of the BHF gaps at densities slightly above $k_F\approx 2.0\ {\rm fm}^{-1}$ are therefore mostly due to the differences in the $^3P_2$-$^3F_2$ waves of the potentials, but at higher densities the differences between the gap are enhanced by differences in the single-particle potentials. The reader should bear in mind that the single-particle energies contain contributions from partial waves up to $l\leqslant 10$. The largest differences arise, however, from contributions from the $^1S_0$ and $^3P_2$-$^3F_2$ partial waves; see also the discussion in Ref. [25]. An extreme case is again the gap obtained with Nijm-II. It is caused by the very attractive $^3P_2$ matrix elements, amplified by the fact that the effective mass starts to increase at densities above $k_F\approx 2.5\,{\rm fm}^{-1}$ with this potential.

Finally, in the lower panel of Fig. 4, we illustrate the effect of different approximation schemes with an individual *NN* potential (CD-Bonn); namely, we compare the energy gaps obtained with the free single-particle spectrum, the BHF spectrum, and an effective mass approximation,

$$e(k)=U_0+\frac{k^2}{2m^*}, \tag{12}$$

where $m^*$ is given in Eq. (11). In addition, also the gap in the uncoupled $^3P_2$ channel, i.e., neglecting the tensor coupling, is shown.

It becomes clear from Fig. 4 that the BHF spectrum forces a reduction of the gap by about a factor of 2–3. However, an effective mass approximation should not be used when calculating the gap, because details of the single-particle spectrum around the Fermi momentum are important in order to obtain a correct value. The single-particle energies in the effective mass approximation are too steep near $k_F$. We also emphasize that it is important to solve the coupled $^3P_2$-$^3F_2$

gap equations. By turning off the $^3P_2$-$^3F_2$ and $^3F_2$ channels, one obtains a $^3P_2$ gap that is considerably lower than the $^3P_2$-$^3F_2$ one. The reduction varies with the potential, due to different strengths of the tensor force. For more detailed discussions of the importance of the tensor force, the reader is referred to Refs. [9,11,12].

### B. Hints from the $^3P_2$ phase shifts

The first calculation of the $^3P_2$ gap in neutron matter was carried out by Hoffberg *et al.* [28] in 1970. They used the weak-coupling expression for the energy gap to express it in terms of the $^3P_2$ phase shifts available at that time, and obtained a maximum gap of around 1 MeV at $k_F \approx 2.3$ fm$^{-1}$. Since all interactions considered in the present paper are fitted in the energy range 0–350 MeV, it would be interesting to use the recent phase-shift analysis by Arndt *et al.* [27] to get some hints on the behavior of the energy gap at higher densities. The phase shifts determine the interaction only on the energy shell; so to go from these ''experimental'' points to the energy gaps, we must make some rather strong assumptions.

First of all, we switch off the interaction in the $^3F_2$ and $^3P_2$-$^3F_2$ channels and consider pure $^3P_2$ pairing. We are then left with only one gap equation to solve, and when we use the angle average approximation it is identical in form to the equation for $^1S_0$ pairing:

$$\Delta_1(k) = -\frac{1}{\pi}\int_0^\infty dk' k'^2 V_{11}(k,k') \frac{\Delta_1(k')}{E(k')}. \tag{13}$$

In a recent paper [4] two of the authors derived an expression for the $^1S_0$ gap in neutron and nuclear matter in terms of the phase shifts in this partial wave. This was possible because the interaction in this channel is to a good approximation rank-1 separable at low energies due to the $^1S_0$ two-nucleon virtual state [3,29]. No resonance or virtual state exists in the $^3P_2$ channel, but we will nevertheless approximate the interaction in this channel by a rank-1 separable form

$$V_{11}(k,k') = \lambda v(k) v(k'), \tag{14}$$

where $\lambda$ is a constant. The interaction can then be expressed in terms of the phase shifts as [4,30]

$$\lambda v^2(k) = -\frac{\sin\delta(k)}{k} e^{-\alpha(k)}, \tag{15}$$

where $\alpha(k)$ is given by a principle value integral

$$\alpha(k) = \frac{1}{\pi} P \int_{-\infty}^{+\infty} dk' \frac{\delta(k')}{k'-k}, \tag{16}$$

and the phase shifts $\delta(k)$ are extended to negative momenta through $\delta(-k) = -\delta(k)$. This prescription works only for a purely attractive or purely repulsive interaction. The $^3P_2$ phase shifts change sign at $E_{\rm lab} \approx 1100$ MeV, and thus the interaction goes from attractive to repulsive at this energy. We therefore cut the integral in Eq. (16) at $k \approx 3.6$ fm$^{-1}$, which corresponds to $E_{\rm lab} \approx 1100$ MeV. For a rank-1 separable interaction, the solution of Eq. (13) is given by $\Delta_F v(k)$, where $\Delta_F$ is the gap at the Fermi momentum found by solving

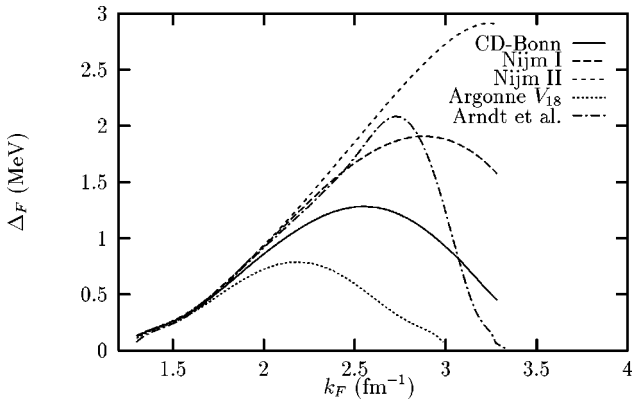


FIG. 6. $^3P_2$ gap calculated with separable potentials constructed directly from the $^3P_2$ phase shifts.

$$\frac{1}{\pi}\int_0^\infty dk' k'^2 \frac{\lambda v^2(k')}{E(k')} = -1. \tag{17}$$

Using phase shifts from the analysis of Arndt *et al.* [27,31], we constructed an interaction for the $^3P_2$ channel according to the prescription above, and then proceeded to solve Eq. (17) for $\Delta_F$. The results are shown in Fig. 6. For comparison we also display the results of the following calculation for the various potentials: we took the phase shifts at energies up to 1100 MeV computed earlier and shown in Fig. 1. From these we constructed a rank-1 separable approximation to the $^3P_2$ wave of the various potentials, as described above, and then used this to solve the gap equation. As such, we have an as close as possible link with the calculation based solely on the phase shifts of Arndt *et al.* [27,31]. This allows us in turn to see directly the consequences of the failure of the potentials to fit the high-energy $^3P_2$ phase shifts. When looking at Fig. 6 and reading the following discussion, one should bear in mind that the gap has an exponential dependence on the interaction; so quite small differences in the matrix elements of the interaction can be translated into large differences in the energy gap. But this also makes the gap a good quantity to use when comparing interactions, as any difference is magnified.

Although the approximation made here should not be taken too seriously, the results indicate some important conclusions about the $^3P_2$ waves of the recent nucleon-nucleon interactions. All seem to have about the right amount of attraction at densities below $k_F \approx 2.0$ fm$^{-1}$. Between $k_F \approx 2.0$ fm$^{-1}$ and $k_F \approx 3.0$ fm$^{-1}$ all interactions except Nijm-II seem to be a bit too repulsive. Above $k_F \approx 3.0$, Argonne $V_{18}$ is probably too repulsive, while Nijm-I and -II are most certainly too attractive, and the same probably also holds for the CD-Bonn. If one uses the weak-coupling expression for the gap,

$$\Delta_F \approx 2\epsilon_F e^{-V_{11}(k_F,k_F)/N(0)}, \tag{18}$$

where $\epsilon_F$ is the Fermi energy and $N(0)$ the density of states at the Fermi level, one sees that the gap vanishes where the

interaction goes to zero. In our phase-shift approximation, this happens where the phase shifts change sign, at $k_F \approx 3.6$ fm$^{-1}$. The Argonne $V_{18}$ gap then seems to disappear somewhat too early, while the other potentials give gaps which exist up to what are probably unrealistically high densities.

## VI. CONCLUSION

We have presented new calculations of the pairing gap in the $^3P_2$-$^3F_2$ channel for pure neutron matter as a function of density. With these calculations we have aimed at establishing on a firm basis the numerical value of the gap once the bare nucleon-nucleon interaction is used as the pairing interaction, since in this context contradictory results have been presented in the literature. Three different numerical methods to solve the pairing gap have been employed in this paper. Since all three methods gave the same results, the pairing gaps we have obtained should be reliable from a technical point of view.

However, our calculations have revealed that the behavior of the $^3P_2$-$^3F_2$ gap at densities above $k_F \approx 2.0$ fm$^{-1}$, corresponding to $\rho \approx 1.7\rho_0$, where $\rho_0$ is the nuclear matter saturation density, must be considered as largely unknown. Up to this point the gap is increasing (the values at $k_F = 2.0$ fm$^{-1}$ are about 0.6 MeV with free single-particle spectrum, and about 0.3 MeV with BHF spectrum, independent of the potential), but how far in density this increase continues depends on the individual potentials, in line with their extrapolations of the $^3P_2$ phase-shift predictions. Bearing in mind that the Nijm-II potential fitted the empirical $^3P_2$ phase shift rather well up to $E_{\rm lab} \approx 600$ MeV ($k_F \approx 2.7$ fm$^{-1}$), we can deduce from Fig. 4 that the maximum gap with a free spectrum is probably below 1 MeV. How high up in density the gap exists must be left as an open question, although the phase shifts indicate that the gap should disappear at around $k_F = 3.6\,\text{fm}^{-1}$, corresponding to $\rho \approx 10\rho_0$. At this point also the purely nucleonic treatment of the dense medium is surely inappropriate.

Before a precise calculation of the $^3P_2$-$^3F_2$ pairing gap can be made, one therefore needs a nucleon-nucleon potential that fits the phase shifts up to $E_{\rm lab} \approx 1$ GeV accurately. To us, the construction of potential models, in which the inelasticities above $E_{\rm lab} = 350\,\text{MeV}$ due to the opening of the $N\Delta$ channel are taken into account, seems to be more urgent than the evaluation of polarization effects on the $^3P_2$-$^3F_2$ gap with the existing potential models.

## ACKNOWLEDGMENTS

We would like to thank John Clark, Umberto Lombardo, and Eivind Osnes for interesting discussions. Thanks are also due to Ruprecht Machleidt for providing us with useful information about potentials and phase shifts in the $^3P_2$ wave.

[1] J. A. Sauls, in *Timing Neutron Stars*, edited by H. Ögelman and E. P. J. van den Heuvel (Dordrecht, Kluwer, 1989), p. 457.
[2] M. Baldo, J. Cugnon, A. Lejeune, and U. Lombardo, Nucl. Phys. **A515**, 409 (1990).
[3] V. A. Kodel, V. V. Kodel, and J. W. Clark, Nucl. Phys. **A598**, 390 (1996).
[4] Ø. Elgarøy and M. Hjorth-Jensen, Phys. Rev. C **57**, 1174 (1998).
[5] H.-J. Schulze, J. Cugnon, A. Lejeune, M. Baldo, and U. Lombardo, Phys. Lett. B **375**, 1 (1996).
[6] J. M. C. Chen, J. W. Clark, E. Krotschek, and R. A. Smith, Nucl. Phys. **A451**, 509 (1986); J. M. C. Chen, J. W. Clark, R. D. Dave, and V. V. Khodel, *ibid.* **A555**, 59 (1993).
[7] T. L. Ainsworth, J. Wambach, and D. Pines, Phys. Lett. B **222**, 173 (1989); J. Wambach, T. L. Ainsworth, and D. Pines, Nucl. Phys. **A555**, 128 (1993).
[8] S. Tsuruta, Phys. Rep. **292**, 1 (1998).
[9] L. Amundsen and E. Østgaard, Nucl. Phys. **A437**, 487 (1985).
[10] M. Baldo, J. Cugnon, A. Lejeune, and U. Lombardo, Nucl. Phys. **A536**, 349 (1992).
[11] T. Takatsuka and R. Tamagaki, Prog. Theor. Phys. Suppl. **112**, 27 (1993).
[12] Ø. Elgarøy, L. Engvik, M. Hjorth-Jensen, and E. Osnes, Nucl. Phys. **A607**, 425 (1996).
[13] V. V. Khodel, Ph.D. thesis, Washington University, St. Louis, 1997; V. A. Khodel, V. V. Khodel, and J. W. Clark, Phys. Rev. Lett. (submitted).
[14] R. B. Wiringa, V. G. J. Stoks, and R. Schiavilla, Phys. Rev. C **51**, 38 (1995).
[15] R. Machleidt, F. Sammarruca, and Y. Song, Phys. Rev. C **53**, 1483 (1996).
[16] V. G. J. Stoks, R. A. M. Klomp, C. P. F. Terheggen, and J. J. de Swart, Phys. Rev. C **48**, 792 (1993).
[17] M. Lacombe *et al.*, Phys. Rev. C **21**, 861 (1980).
[18] R. B. Wiringa, R. A. Smith, and T. L. Ainsworth, Phys. Rev. C **29**, 1207 (1984).
[19] R. Machleidt, Adv. Nucl. Phys. **19**, 189 (1989).
[20] M. Baldo, U. Lombardo, and P. Schuck, Phys. Rev. C **52**, 975 (1995).
[21] See, e.g., J. R. Schrieffer, *Theory of Superconductivity* (Addison-Wesley, New York, 1964), p. 248.
[22] J. P. Jeukenne, A. Lejeune, and C. Mahaux, Phys. Rep., Phys. Lett. **25C**, 83 (1976).
[23] E. Krotscheck, Z. Phys. **251**, 135 (1972).
[24] V. G. J. Stoks, R. A. M. Klomp, M. C. M. Rentmeester, and J. J. de Swart, Phys. Rev. C **48**, 792 (1993).
[25] L. Engvik, M. Hjorth-Jensen, R. Machleidt, H. Müther, and A. Polls, Nucl. Phys. **A627**, 85 (1997).
[26] R. Machleidt, K. Holinde, and Ch. Elster, Phys. Rep. **149**, 1 (1987).
[27] R. A. Arndt, C. H. Oh, I. I. Strakovsky, R. L. Workman, and F. Dohrmann, Phys. Rev. C **56**, 3005 (1997).
[28] M. Hoffberg, A. E. Glassgold, R. W. Richardson, and M. Ruderman, Phys. Rev. Lett. **24**, 775 (1970).
[29] B. V. Carlson, T. Frederico, and F. B. Guimarães, Phys. Rev. C **56**, 3097 (1997).
[30] G. E. Brown and A. D. Jackson, *The Nucleon-Nucleon Interaction* (North-Holland, Amsterdam, 1976).
[31] R. A. Arndt, ''Interactive Dial-in Program SAID'' (URL http://clsaid.phys.vt.edu/%7ECAPS/).